MOX–Report No. 10/2013

A stream virtual element formulation of the Stokes problem on polygonal meshes

Antonietti, P.F.; Beirao da Veiga, L.; Mora, D.; Verani, M.

MOX, Dipartimento di Matematica "F. Brioschi"
Politecnico di Milano, Via Bonardi 9 - 20133 Milano (Italy)

mox@mate.polimi.it http://mox.polimi.it

A stream virtual element formulation of the Stokes problem on polygonal meshes

Paola F. Antonietti[a], Lourenco Beirão da Veiga[b], David Mora[c] and Marco Verani[d]

February 25, 2013

[a] MOX, Dipartimento di Matematica, Politecnico di Milano
Piazza Leonardo da Vinci 32, I-20133 Milano, Italy
E-mail: paola.antonietti@polimi.it

[b] Dipartimento di Matematica, Università di Milano
Via Saldini 50, I-20133 Milano, Italy
E-mail: lourenco.beirao@unimi.it

[c] Departamento de Matemática, Universidad del Bío-Bío, Casilla 5-C, Concepción, Chile
and CI^{2}MA, Universidad de Concepción, Concepción, Chile
E-mail: dmora@ubiobio.cl

[d] MOX, Dipartimento di Matematica, Politecnico di Milano
Piazza Leonardo da Vinci 32, I-20133 Milano, Italy
E-mail: marco.verani@polimi.it

Abstract

In this paper we propose and analyze a novel stream formulation of the Virtual Element Method (VEM) for the solution of the Stokes problem. The new formulation hinges upon the introduction of a suitable stream function space (characterizing the divergence free subspace of discrete velocities) and it is equivalent to the velocity-pressure (inf-sup stable) mimetic scheme presented in [8] (up to a suitable reformulation into the VEM framework). Both schemes are thus stable and linearly convergent but the new method results to be more desirable as it employs much less degrees of freedom and it is based on a positive definite algebraic problem. Several numerical experiments assess the convergence properties of the new method and show its computational advantages with respect to the mimetic one.

1 Introduction

Various approaches to extend finite element methods to non-traditional elements (general polygons, pyramids, polyhedra, etc.) have been developed over the last period, see e.g.[24, 25, 26, 27]. The construction of basis functions for such elements is a challenging task and may require extensive geometrical analysis. The mimetic finite difference (MFD) method [16, 17, 14, 5] works on general polygonal meshes and preserve the fundamental properties of the underlying physical and mathematical models. Thanks to its great flexibility, the MFD method has been applied successfully to a wide range of problems, see for instance also [2, 1, 3, 8, 12] and the review paper [23] for a much longer list. Very recently, a new evolution of

MFD was proposed in [7], taking the name of Virtual Element Method (VEM). The VEM takes the steps from the main ideas of modern mimetic schemes but follows a Galerkin discretization of the problem, and therefore can be fully interpreted as a generalization of the finite element (FE) method. Thus, the VEM couples the flexilibity of mimetic methods with the theoretical and applicative background of FE methods. Since the VEM are very recent, the present published literature is limited to [7, 18, 6, 11].

A fundamental role in applied problems is represented by the study of reliable and effective numerical methods for fluids. In particular, the simulation of Stokes flows (characterized by very small Reynolds number) represents a standalone important problem (e.g. in the context of the numerical simulation of the blood flow) and a crucial step towards the simulation of more complex fluids, such as sedimentation processes. FE methods constitute a classical choice to accomplish this goal, see e.g. [19, 21]. Traditionally, FE methods rely on triangular (simplicial) and quadrilateral meshes. However, in complex simulations one often encounters general polygonal and polyhedral meshes (see e.g. [24]). In [8, 9, 10] new MFD methods for the Stokes problem on polygonal meshes have been introduced and analyzed.

In this paper we propose and analyze a novel stream formulation of the Virtual Element Method for the solution of the Stokes problem. The new formulation hinges upon the introduction of a suitable stream function space (characterizing the divergence free subspace of discrete velocities). we show that the VEM velocity-pressure scheme of the Stokes problem (which is a reformulation of the MFD method introduced in [8]) is equivalent to our VEM stream formulation. Using general assumptions on the computational domain, we establish that both schemes are well posed and we prove linear convergence for the methods.

The outline of this article is as follows: In Section 2, we discuss the variational formulation of the Stokes problem. In Section 3 we recast into the VEM framework the velocity-pressure (inf-sup stable) mimetic scheme presented in [8]. In Section 4 we introduce our novel stream formulation and we prove its equivalence with the velocity-pressure virtual element formulation: both schemes are proved to be stable and linearly convergent. Finally, in Section 5 we assess the convergence properties of the new stream method and show its computational advantages with respect to the original one based on the velocity pressure formulation.

Throughout the paper, we will follow the usual notation for Sobolev spaces and norms (see e.g. [20]). In particular, for an open bounded domain $\mathcal{D}$, we will use $|\cdot|_{s,\mathcal{D}}$ and $\|\cdot\|_{s,\mathcal{D}}$ to denote seminorm and norm, respectively, in the Sobolev space $H^s(\mathcal{D})$, while $(\cdot,\cdot)_{\mathcal{D}}$ will denote the $L^2(\mathcal{D})$ inner product. Often the subscript will be omitted when $\mathcal{D}$ is the computational domain Ω. Moreover, for any subset $\mathcal{D} \subseteq \mathbb{R}^2$ and non-negative integer k, we indicate by $\mathbb{P}_k(\mathcal{D})$ the space of polynomials of degree up to k defined on $\mathcal{D}$. Finally, C will be a generic constant independent of the decomposition that could change from an occurrence to the other.

2 The Stokes Problem

Let $\Omega \subset \mathbb{R}^2$ be a polygonal domain. We consider the two dimensional Stokes problem

$$\begin{cases} -\mathbf{div}(\nu \boldsymbol{\nabla}^S \mathbf{u}) - \nabla p = \mathbf{f} & \text{in } \Omega \\ \operatorname{div} \mathbf{u} = 0 & \text{in } \Omega \\ \mathbf{u} = \mathbf{0} & \text{on } \partial\Omega, \end{cases} \tag{1}$$

where the symbols $\mathbf{div}, \mathrm{div}, \nabla, \boldsymbol{\nabla}^S$ represent the vector divergence, the divergence, the gradient and the symmetric gradient operator, respectively. The given external force $\mathbf{f}$ is assumed in $[L^2(\Omega)]^2$, while the scalar field ν is uniformly bounded and strictly positive on the domain Ω. As usual, the vector field $\mathbf{u}$ represents the velocities and the scalar field p the pressures.

Let $L^2_0(\Omega)$ denote the space of L^2 functions with zero average. Introducing the bilinear form $a(\mathbf{u}, \mathbf{v}) := (\nu \boldsymbol{\nabla}^S \mathbf{u}, \boldsymbol{\nabla}^S \mathbf{v})$ the variational formulation of the Stokes problem reads

$$\begin{cases} \text{Find } \mathbf{u} \in V := [H^1_0(\Omega)]^2, \ p \in Q := L^2_0(\Omega) \text{ such that} \\ a(\mathbf{u}, \mathbf{v}) + (\mathrm{div}\, \mathbf{v}, p) = (\mathbf{f}, \mathbf{v}) \qquad \forall \mathbf{v} \in V \\ (\mathrm{div}\, \mathbf{u}, q) = 0 \qquad \forall q \in Q \end{cases} \tag{2}$$

It is well known that problem (2) has a unique solution, see for instance [21].

Let us introduce the space of divergence-free functions

$$Z = \{\mathbf{v} \in V : \mathrm{div}\, \mathbf{v} = 0\}$$

and notice that the solution $\mathbf{u} \in V$ to problem (2) is determined by solving the following problem

$$\begin{cases} \text{Find } \mathbf{u} \in Z \text{ such that} \\ a(\mathbf{u}, \mathbf{v}) = (\mathbf{f}, \mathbf{v}) \qquad \forall \mathbf{v} \in Z. \end{cases} \tag{3}$$

Under the assumption that Ω is a two-dimensional simply connected domain, it is well known that for every $\mathbf{v} \in Z$ there exists a uniquely defined scalar potential function $w \in H^2(\Omega)/\mathbb{R}$ (see for instance [21]) such that:

$$\mathbf{v} = \mathbf{curl}\, w$$

where $\mathbf{curl} = (\frac{\partial}{\partial y}, -\frac{\partial}{\partial x})$. Setting

$$\Phi = \{\varphi \in H^2(\Omega)/\mathbb{R} \text{ such that } \mathbf{curl}\, \varphi = \mathbf{0}\}$$

we can write the solution $\mathbf{u}$ of (3) as $\mathbf{u} = \mathbf{curl}\, \psi$ where $\psi \in \Phi$ is solution of the following problem

$$\begin{cases} \text{Find } \psi \in \Phi \text{ such that} \\ a(\mathbf{curl}\, \psi, \mathbf{curl}\, \varphi) = (\mathbf{f}, \mathbf{curl}\, \varphi) \qquad \forall \varphi \in \Phi. \end{cases} \tag{4}$$

We will refer to (4) as to the stream function formulation of the Stokes problem (2).

3 VEM for Stokes (I): velocity-pressure formulation

In this section we recast the Mimetic Finite Difference (MFD) method analyzed in [8, 10] for the numerical approximation of the Stokes problem into the framework of the Virtual Element Method (VEM) recently introduced in [7].

Let $\{\mathcal{T}_h\}_h$ be a sequence of decompositions of Ω into elements K, let $\mathcal{V}_h$ be the set of mesh vertexes, $\mathcal{V}_h^b$ the set of boundary vertexes and let $\mathcal{E}_h$ be the set of edges e of $\mathcal{T}_h$. We assume that for every h, the decomposition $\mathcal{T}_h$ is made of a finite number of *simple polygons* (i.e. open simply connected sets with non-self intersecting boundaries made of a finite number

of straight line segments). For all $e \in \mathcal{E}_h$ we associate once and for all a normal unit vector $\mathbf{n}_e$ and a tangent unit vector $\mathbf{t}_e$ obtained by an anti-clockwise rotation of $\mathbf{n}_e$. Moreover, we denote by $\mathcal{E}_K$ the set of edges of K.

The bilinear form $a(\cdot,\cdot)$ can obviously be split as

$$a(\mathbf{u},\mathbf{v}) = \sum_{K\in\mathcal{T}_h} a^K(\mathbf{u},\mathbf{v}) \qquad \forall\, \mathbf{u},\, \mathbf{v} \in V, \quad a^K(\mathbf{u},\mathbf{v}) := (\nu \boldsymbol{\nabla}^S \mathbf{u}, \boldsymbol{\nabla}^S \mathbf{v})_K, \tag{5}$$

with $(\cdot,\cdot)_K$ representing the L^2 scalar product on K.

In the following sections, we will show that for each $h > 0$ it is possible to build:

1. a couple of spaces (V_h, Q_h) with $V_h \subset V$ and $Q_h \subset Q$;
2. a symmetric bilinear form a_h from $V_h \times V_h$ to $\mathbb{R}$ which can be split as

$$a_h(\mathbf{u}_h,\mathbf{v}_h) = \sum_{K\in\mathcal{T}_h} a_h^K(\mathbf{u}_h,\mathbf{v}_h) \quad \forall\, \mathbf{u}_h,\, \mathbf{v}_h \in V_h, \tag{6}$$

   where $a_h^K(\cdot,\cdot)$ is a bilinear form on $V_{h|K} \times V_{h|K}$;
3. an element $\mathbf{f}_h \in V_h'$ and a discrete duality pair $\langle\cdot,\cdot\rangle_h$;

in such a way that the resulting discrete problem

$$\begin{cases} \text{Find } \mathbf{u}_h \in V_h,\ p_h \in Q_h \text{ such that} \\ a_h(\mathbf{u}_h,\mathbf{v}_h) + (\operatorname{div}\mathbf{v}_h, p_h) = \langle \mathbf{f}_h, \mathbf{v}_h\rangle_h \qquad \forall \mathbf{v}_h \in V_h \\ (\operatorname{div}\mathbf{u}_h, q_h) = 0 \qquad \forall q_h \in Q_h, \end{cases}$$

has a unique solution $\mathbf{u}_h, p_h$ and exhibits optimal approximation properties.

3.1 Discrete spaces for velocities and pressures

We first construct the local discrete velocity space $V_{h|K}$, $K \in \mathcal{T}_h$. To this aim, we preliminary introduce the local space $\mathcal{H}(K) \subset [H^1(K)]^2$ made of vector functions with constant divergence

$$\mathcal{H}(K) = \Big\{ \mathbf{v} \in [H^1(K)]^2 \ :\ |K| \operatorname{div}\mathbf{v} = \big(\int_{\partial K} \mathbf{v}\cdot\mathbf{n}_e^K \,\mathrm{d}s\big) \text{ in } K \Big\},$$

being $\mathbf{n}_e^K$ the outward unit normal to K. Then, we define the finite dimensional space $V_{h|K}$ as

$$V_{h|K} = \big\{ \mathbf{v} \in \mathcal{H}(K) \ :\ \mathbf{v} \text{ minimizes } ||\nabla\mathbf{v}||^2_{L^2(K)}, \mathbf{v} \in \mathbb{B}(\partial K) \big\}, \tag{7}$$

where

$$\mathbb{B}(\partial K) = \big\{ \mathbf{v} \in [C^0(\partial K)]^2 \ :\ \mathbf{v}_{|e}\cdot\mathbf{t}_e^K \in \mathbb{P}_1(e),\ \mathbf{v}_{|e}\cdot\mathbf{n}_e^K \in \mathbb{P}_2(e)\ \forall e \in \mathcal{E}_K \big\},$$

where $\mathbf{t}_e^K$ is the tangent vector defined as the counterclockwise rotation of $\mathbf{n}_e^K$ by $90°$. Note that the space $V_{h|K}$ is well defined. Indeed, given a (piecewise polynomial) boundary value $\mathbf{v}|_{\partial K} \in [H^{1/2}(\partial K)]^2$, the associated function $\mathbf{v}$ inside the element K is obtained by solving

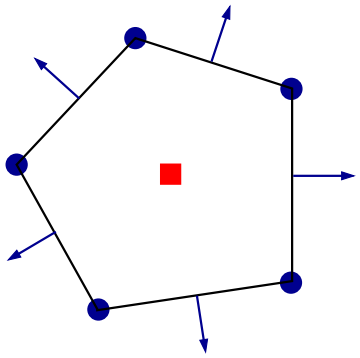

Figure 1: Local degrees of freedom for velocities (blue) and pressures (red). The blue dots represent (vector) point values at vertexes, while the arrows represent the point value of the normal component at the midpoint of the edge. The square represents the average.

the following well posed Stokes-type problem

$$\begin{cases} \text{Find } \mathbf{v} \in [H^1(K)]^2, r \in L^2_0(K) \ \text{ such that} & \\ -\Delta \mathbf{v} - \nabla r = \mathbf{0} & \text{in } K \\ \operatorname{div} \mathbf{v} = c & \text{in } K \\ \mathbf{v} \text{ assigned on } \partial K, & \end{cases} \tag{8}$$

where the equations are to be intended in the weak sense and the constant $c := (\int_{\partial K} \mathbf{v} \cdot \mathbf{n}_K \, \mathrm{d}s)/|K|$ is compatible with the boundary conditions.

We remark that the space $V_{h|K}$ contains H^1 vector fields characterized by: (a) linear tangent component and quadratic normal component on each edge e; (b) constant divergence value on K; (c) minimum energy. Moreover, we note that, by standard regularity results for the Stokes problem, the functions in $V_{h|K}$ turn out to be continuous in $\bar{K}$.

It is important to observe that, since the functions of $V_{h|K}$ are uniquely identified by their boundary values, the dimensions of $V_{h|K}$ and $(V_{h|K})_{|\partial K}$ are equal, i.e. $\dim(V_{h|K}) = 3n$, being n the number of edges of K. This leads to introduce the following $3n$ *degrees of freedom* for the space $V_{h|K}$ (cfr. the blue symbols in Figure 1):

- the (vector) values of $\mathbf{v}$ at the *vertexes* of K;
- the values of the normal components $\mathbf{v} \cdot \mathbf{n}_e^K$ at the midpoint of each *edge* of K.

Finally, it is immediate to verify that these degrees of freedom uniquely identify the restriction to ∂K of the functions belonging to $V_{h|K}$.

The global velocity space V_h is obtained by combining the local spaces $V_{h|K}$ accordingly to the local degrees of freedom, as is standard in finite elements [20, 15, 13], and considering the homogeneous boundary conditions. We obtain the space

$$V_h = \{\mathbf{v}_h \in C^0(\Omega) \ : \ \mathbf{v}_h|_K \in V_{h|K} \, \forall K \in \mathcal{T}_h, \ \mathbf{v}_h = \mathbf{0} \text{ on } \partial\Omega\}$$

with the degrees of freedom given by the (vector) values at all the internal vertexes of $\mathcal{T}_h$ and the normal components $\mathbf{v} \cdot \mathbf{n}_e$ at the midpoints of all internal edges e of the mesh.

The pressure space is simply given by the piecewise constant functions

$$Q_h = \{q_h \in L^2_0(\Omega) \ : \ q_h|_K \in \mathbb{P}_0(K) \ \forall K \in \mathcal{T}_h\}$$

and the degrees of freedom are one per element, given by the value of the function on the element (cfr. the red square in Figure 1).

3.2 Bilinear form and loading term

In this section we will discuss the construction of the local bilinear form appearing in (6). For simplicity, we assume that the scalar field ν is piecewise constant with respect to the mesh $\mathcal{T}_h$ and we denote by ν_K the restriction of ν to the element K. The more general situation can be handled by introducing the piecewise approximation $\nu_K = (\int_K \nu \, \mathrm{d}x)/|K|$ of ν.

The local bilinear forms $a_h^K(\cdot,\cdot) : V_{h|K} \times V_{h|K} \to \mathbb{R}$, $K \in \mathcal{T}_h$, are assumed to be symmetric and to satisfy the following *consistency* and *stability* assumptions.

(A1) Consistency: for all $h > 0$ and for all $K \in \mathcal{T}_h$ it holds

$$a_h^K(\mathbf{p}, \mathbf{v}_h) = a^K(\mathbf{p}, \mathbf{v}_h) \qquad \forall \mathbf{p} \in [\mathbb{P}_1(K)]^2, \mathbf{v}_h \in V_{h|K}. \tag{9}$$

(A2) Stability: there exist two positive constants α_* and α^*, independent of h and of K, such that

$$\alpha_* \, a^K(\mathbf{v}_h, \mathbf{v}_h) \le a_h^K(\mathbf{v}_h, \mathbf{v}_h) \le \alpha^* \, a^K(\mathbf{v}_h, \mathbf{v}_h) \qquad \forall \mathbf{v}_h \in V_{h|K}. \tag{10}$$

First of all, we observe that the local degrees of freedom allow us to compute exactly $a^K(\mathbf{p}, \mathbf{v}_h)$ for any $\mathbf{p} \in [\mathbb{P}_1(K)]^2$ and for any $\mathbf{v}_h \in V_{h|K}$. Indeed,

$$\begin{aligned} a^K(\mathbf{p}, \mathbf{v}_h) &= \nu_K \int_K \boldsymbol{\nabla}^S \mathbf{p} : \boldsymbol{\nabla}^S \mathbf{v}_h \, \mathrm{d}x \\ &= -\nu_K \int_K \mathbf{div}(\boldsymbol{\nabla}^S \mathbf{p}) \cdot \mathbf{v}_h \, \mathrm{d}x + \nu_K \int_{\partial K} ((\boldsymbol{\nabla}^S \mathbf{p}) \mathbf{n}_e^K) \cdot \mathbf{v}_h \, \mathrm{d}s, \end{aligned} \tag{11}$$

with $\mathbf{n}_e^K$ the outward unit normal to K. Therefore, since $\mathbf{div}(\boldsymbol{\nabla}^S \mathbf{p}) = \mathbf{0}$ and the functions $\mathbf{v}_h \in V_{h|K}$ are known explicitly on the boundary, the right hand side of (9) can be computed exactly without knowing $\mathbf{v}_h$ in the interior of K.

We note that the practical implementation of the local stiffness matrices associated to the local bilinear forms $a_h(\cdot,\cdot)$ can be found, for the mimetic framework, in [8] or can be easily adapted by extending the VE construction of [7] to the present case. Detailing such a construction is beyond the scope of the present paper. However, we remark that, in order for condition (10) to hold ($h-$uniformly), some mesh regularity assumptions are needed. A possible choice, although not the more general one, is the following [7].

(A3) Mesh regularity: there exists a constant $\gamma > 0$ such that for any $h > 0$ every element $K \in \mathcal{T}_h$ is star-shaped with respect to a ball of radius $\ge \gamma h_K$, being h_K the diameter of K. Moreover, we assume that there exists a constant $\gamma' > 0$ such that for any $h > 0$ and for every $K \in \mathcal{T}_h$, the distance between any two vertexes of K is $\ge \gamma' h_K$.

We now discuss the construction of the *loading term*. For every $K \in \mathcal{T}_h$ and $\mathbf{v}_h \in V_{h|K}$ we set

$$\overline{\mathbf{v}}_K := \frac{1}{n}\sum_{i=1}^{n} \mathbf{v}_h(\mathsf{v}_i), \quad \mathsf{v}_i = \text{vertexes of } K. \tag{12}$$

We approximate $\mathbf{f}$ by a piecewise constant $\mathbf{f}_h$ and we denote by $\mathbf{f}_K$ the restriction of $\mathbf{f}_h$ to K. For instance, the value $\mathbf{f}_K$ can be chosen as the average of $\mathbf{f}$ on K. This naturally leads to identify $\mathbf{f}_h$ with an element of the dual space V_h' and to introduce the following duality pair

$$\langle \mathbf{f}_h, \mathbf{v}_h \rangle_h := \sum_{K\in\mathcal{T}_h} \int_K \mathbf{f}_K \cdot \overline{\mathbf{v}}_K \, \mathrm{d}x = \sum_{K\in\mathcal{T}_h} |K| \mathbf{f}_K \cdot \overline{\mathbf{v}}_K. \tag{13}$$

3.3 Discrete problem

The results of the previous sections allow to introduce the following virtual element method in velocity-pressure formulation for the approximation of the Stokes problem (1):

$$\begin{cases} \text{Find } \mathbf{u}_h \in V_h, \ p_h \in Q_h \text{ such that} \\ a_h(\mathbf{u}_h, \mathbf{v}_h) + (\operatorname{div} \mathbf{v}_h, p_h) =< \mathbf{f}_h, \mathbf{v}_h >_h \qquad \forall \mathbf{v}_h \in V_h \\ (\operatorname{div} \mathbf{u}_h, q_h) = 0 \qquad \forall q_h \in Q_h. \end{cases} \tag{14}$$

We preliminary remark that the divergence of any function $\mathbf{v}_h$ in $V_{h|K}$ is explicitly computable. Indeed, since $\operatorname{div} \mathbf{v}_h|_K$ is constant, we have

$$\operatorname{div} \mathbf{v}_h|_K = \frac{1}{|K|}\int_K \operatorname{div} \mathbf{v}_h \, \mathrm{d}x = \frac{1}{|K|}\int_{\partial K} \mathbf{v}_h \cdot \mathbf{n}_e^K \, \mathrm{d}s, \tag{15}$$

where the right hand side is computable as the functions in $V_{h|K}$ are explicitly known on the boundary. Hence, recalling that the functions in Q_h are constant on each element, the divergence terms appearing in (14) are explicitly computable as there holds

$$(\operatorname{div} \mathbf{v}_h, q_h) = \sum_{K\in\mathcal{T}_h} \int_K \operatorname{div} \mathbf{v}_h \, q_h \ \mathrm{d}x = \sum_{K\in\mathcal{T}_h} q_{h|K} \int_K \operatorname{div} \mathbf{v}_h \ \mathrm{d}x$$

for all $\mathbf{v}_h \in V_h$ and $q_h \in Q_h$.

We remark that the VE method (14) is equivalent to the mimetic method for the Stokes problem introduced in [8, 10]. Therefore, stability and convergence results are easily derived from the results in [10] combined with the techniques of [7].

Theorem 3.1 *Let the assumptions* **(A1)-(A3)** *hold for the family of meshes* $\{\mathcal{T}_h\}_{h>0}$. *Then, the problems* (14) *are (uniformly) well posed for all* $h > 0$. *Moreover, let* $(\mathbf{u}, p)$ *be the solution of* (2) *and* $(\mathbf{u}_h, p_h)$ *the solution of* (14) *than it holds*

$$||\mathbf{u} - \mathbf{u}_h||_1 + ||p - p_h||_0 \le C\, h \Big(\sum_{K\in\mathcal{T}_h} (|\mathbf{u}|^2_{2,K} + |\mathbf{f}|^2_{1,K}) \Big)^{1/2},$$

where the constant C *is independent of* h.

4 VEM for Stokes (II): stream formulation

In this section we present our novel virtual element method in stream formulation for the approximation of the Stokes problem (1). The stream formulation hinges upon the introduction of a suitable stream function space (characterizing the divergence free subspace of discrete velocities) and it is equivalent to the velocity-pressure virtual element scheme (14).

Let us first introduce the following space of discrete divergence-free functions

$$\begin{aligned} Z_h &= \left\{ \mathbf{v}_h \in V_h \ : \ \int_\Omega \operatorname{div} \mathbf{v}_h \ q_h \, \mathrm{d}x = 0 \quad \forall q_h \in Q_h \right\} \\ &= \left\{ \mathbf{v}_h \in V_h \ : \ \operatorname{div} \mathbf{v}_h = 0 \right\} , \end{aligned}$$

where the equality above follows from the fact that V_h has piecewise constant divergence. Moreover, we define the following (local) space of discrete stream functions

$$\Phi_h|_K := \left\{ \phi \in H^2(K) : \ \phi \text{ minimizes } \|\nabla(\mathbf{curl}\, \phi)\|^2_{L^2(K)}, \phi \in \mathbb{B}'(\partial K), \ \nabla\phi \in \mathbb{B}''(\partial K) \right\}$$

where

$$\begin{aligned} \mathbb{B}'(\partial K) &= \left\{ v \in C^0(\partial K) \ : \ v_{|e} \in \mathbb{P}_3(e) \ \forall e \in \mathcal{E}_K \right\}, \\ \mathbb{B}''(\partial K) &= \left\{ \mathbf{v} \in [C^0(\partial K)]^2 \ : \ \mathbf{v}_{|e} \cdot \mathbf{n}_e^K \in \mathbb{P}_1(e) \ \forall e \in \mathcal{E}_K \right\}. \end{aligned}$$

Note that the space $\Phi_h|_K$ is well defined. Indeed, given the values on the boundary ∂K, the function ϕ inside the element K is found by solving a fourth order elliptic problem

$$\begin{cases} -\Delta^2 \phi = 0 \qquad \text{in } K \\ \phi \text{ assigned on } \partial K \\ \nabla\phi \cdot \mathbf{n}_e^K \text{ assigned on } \partial K, \end{cases}$$

and standard regularity results for fourth order elliptic problems yields that the functions of $\Phi_h|_K$ are in $C^1(K)$.

It is easy to check that the following constitute a set of degrees of freedom for the space $\Phi_h|_K$ (see Figure 2):

- the point values of ϕ at the vertexes of K;
- the (vector) values of $\nabla\phi$ at the vertexes of K.

The global stream function space Φ_h is obtained by combining the local spaces $\Phi_{h|K}$ accordingly to the local degrees of freedom, taking into account the boundary conditions and enforcing an additional constraint in order to neglect the global constant functions. We obtain the space

$$\Phi_h = \{\phi_h \in C^1(\Omega) \ : \ \phi_h|_K \in \Phi_{h|K} \, \forall K \in \mathcal{T}_h, \ \mathbf{curl}\, \phi_h = \mathbf{0} \text{ on } \partial\Omega, \int_\Omega \phi_h \, \mathrm{d}x = 0\}. \tag{16}$$

We preliminary collect the following result:

Lemma 4.1 *For every $\mathbf{v}_h \in Z_h$ there exists a unique $\phi_h \in \Phi_h$ such that*

$$(\mathbf{curl}\, \phi_h)|_{\partial K} = \mathbf{v}_h|_{\partial K} \qquad \forall K \in \mathcal{T}_h. \tag{17}$$

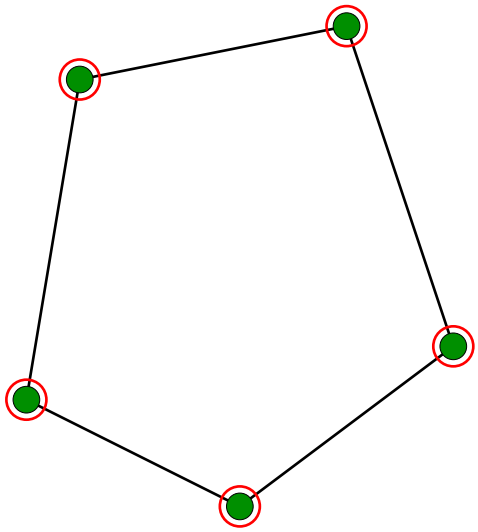

Figure 2: Local degrees of freedom for the stream space Φ_h. Green dots represent point values and red circles denote point values of the gradient.

Proof. Given $\mathbf{v}_h \in Z_h$, we will explicitly build $\phi_h \in \Phi_h$ such that (17) holds. Recalling the degrees of freedom of Φ_h (see Figure 2), we need to determine the values of ϕ_h and $\nabla\phi_h$ at all the mesh vertexes. We preliminary choose an arbitrary vertex $\tilde{\mathsf{v}}$ of the mesh and set $\phi_h(\tilde{\mathsf{v}}) = C$, for some constant C to be chosen later. Then, for any other vertex $\widehat{\mathsf{v}}$ in the mesh, we build an oriented path $\boldsymbol{\gamma}_h$ from $\tilde{\mathsf{v}}$ to $\widehat{\mathsf{v}}$ made of mesh edges and determine the value of ϕ_h at $\widehat{\mathsf{v}}$ as follows:

$$\phi_h(\widehat{\mathsf{v}}) := \phi_h(\tilde{\mathsf{v}}) + \sum_{e\in\boldsymbol{\gamma}_h} \int_e \mathbf{v}_h \cdot \mathbf{n}_e^{\boldsymbol{\gamma}_h}\, \mathrm{d}s, \tag{18}$$

where $\mathbf{n}_e^{\boldsymbol{\gamma}_h}$ is the unit normal to edge e that is obtained by a clockwise rotation of the unit tangent pointing in the direction of the oriented path. We note that the definition (18) is well posed since $\phi_h(\widehat{\mathsf{v}})$ in (18) does not depend on the chosen path. Indeed, $\operatorname{div}\mathbf{v}_h = 0$ and the fact that the domain is simply connected imply that the sum in the right hand side of (18) is zero on any closed path.

As a second step, using the definition of the operator $\mathbf{curl}$, we define the value of $\nabla\phi_h$ at each vertex $\widehat{\mathsf{v}}$ by setting:

$$\begin{aligned} &(\mathbf{curl}\,\phi_h)(\widehat{\mathsf{v}}) := \mathbf{v}_h(\widehat{\mathsf{v}}) \quad \forall \widehat{\mathsf{v}} \in \mathcal{V}_h \setminus \mathcal{V}_h^b \\ &(\mathbf{curl}\,\phi_h)(\widehat{\mathsf{v}}) := \mathbf{0} \qquad \forall \widehat{\mathsf{v}} \in \mathcal{V}_h^b\ . \end{aligned} \tag{19}$$

Finally, the initial constant C is chosen in order to satisfy the zero integral condition in (16).

It is now easy to check that ϕ_h satisfies $(\mathbf{curl}\,\phi_h)|_e = \mathbf{v}_h|_e$ for all edges $e \in \mathcal{E}_h$. Indeed, let e be an edge with extrema v_1 and v_2 (ordered in such a way that $\mathbf{t}_e$ points from v_1 to v_2), then (18) yields

$$\int_e (\mathbf{curl}\,\phi_h)\cdot\mathbf{n}_e\,\mathrm{d}s = \int_e (\nabla\phi_h)\cdot\mathbf{t}_e\,\mathrm{d}s = \phi_h(\mathsf{v}_2) - \phi_h(\mathsf{v}_1) = \int_e \mathbf{v}_h\cdot\mathbf{n}_e\,\mathrm{d}s. \tag{20}$$

To conclude we first observe that $\mathbf{v}_h \cdot \mathbf{n}_e$ and $\mathbf{curl}\,\phi_h \cdot \mathbf{n}_e$ are polynomials of degree 2 on e and they assume the same values at the two extrema $\mathsf{v}_1, \mathsf{v}_2$ (see (19)) and the same integral (see (20)); thus they coincide. Finally, $\mathbf{v}_h \cdot \mathbf{t}_e$ and $\mathbf{curl}\,\phi_h \cdot \mathbf{t}_e$ are equal on e because they are linear functions taking the same values at the extrema (see (19)). This concludes the main assertion of the lemma.

The uniqueness follows easily by the same lines and is thus shown briefly. Let $\mathbf{curl}\, w_h = 0$ for some $w_h \in \Phi_h$, then the gradient values must vanish at all vertexes in $\mathcal{V}_h$ and the same holds for all differences $w_h(\mathsf{v}_1) - w_h(\mathsf{v}_2)$ evaluated at the extrema $\mathsf{v}_1, \mathsf{v}_2$ of any edge $e \in \mathcal{E}_h$. The latter yields that w_h assumes the same constant value; i.e., w_h must be constant on Ω. Finally, this implies that the function w_h vanishes due to the zero average condition in the definition of Φ_h. □

Now, we are ready to prove the following characterization of the space Z_h.

Proposition 4.1 *It holds*

$$Z_h = \mathbf{curl}\,\Phi_h := \{\mathbf{curl}\,\phi_h : \phi_h \in \Phi_h\}\ .$$

Proof. For every $\bar{\mathbf{v}} \in [H^{1/2}(\partial K)]^2$ let us introduce the spaces $X_1^K(\bar{\mathbf{v}})$ and $X_2^K(\bar{\mathbf{v}})$ defined as follows

$$\begin{aligned} X_1^K(\bar{\mathbf{v}}) &:= \{\mathbf{v} \in [H^1(K)]^2 : \operatorname{div}\mathbf{v} = 0 \text{ and } \mathbf{v}|_{\partial K} = \bar{\mathbf{v}}\} \\ X_2^K(\bar{\mathbf{v}}) &:= \{\mathbf{curl}\, w : w \in H^2(K) \text{ and } (\mathbf{curl}\, w)_{\partial K} = \bar{\mathbf{v}}\}\ . \end{aligned}$$

Using well known results on the decomposition of two-dimensional vector fields [21, Theorem 3.1] we deduce

$$X_1^K(\bar{\mathbf{v}}) = X_2^K(\bar{\mathbf{v}}) \quad \forall \bar{\mathbf{v}} \in [H^{1/2}(\partial K)]^2. \tag{21}$$

Setting

$$J_K(\mathbf{w}) := \|\nabla \mathbf{w}\|^2_{L^2(K)} \quad \forall \mathbf{w} \in [H^1(K)]^2$$

and using (21) it is immediate to verify that for every $K \in \mathcal{T}_h$ and for every $\bar{\mathbf{v}} \in [H^{1/2}(\partial K)]^2$ the following minimization problems admit unique solutions and there holds

$$\min_{\mathbf{v} \in X_1^K(\bar{\mathbf{v}})} J_K(\mathbf{v}) = \min_{\mathbf{curl}\, w \in X_2^K(\bar{\mathbf{v}})} J_K(\mathbf{curl}\, w)\ . \tag{22}$$

Using the definitions of the spaces Φ_h and Z_h together with equality (22) we can first observe that given

$$\mathbf{v}_h \in V_{h|K} \text{ with } \operatorname{div}\mathbf{v}_h = 0 \quad \text{and} \quad w_h \in \Phi_h|_K$$

such that $(\mathbf{curl}\, w_h)|_{\partial K} = \mathbf{v}_h|_{\partial K}$ we have

$$\mathbf{curl}\, w_h = \mathbf{v}_h \text{ in } K. \tag{23}$$

From the definition of the spaces it easily follows that for each $w_h \in \Phi_h$ it exists a unique $\mathbf{v}_h \in V_h$ such that $(\mathbf{curl}\, w_h)|_{\partial K} = \mathbf{v}_h|_{\partial K}$ for all $K \in \mathcal{T}_h$, and such $\mathbf{v}_h$ must satisfy $\operatorname{div}\mathbf{v}_h = 0$. Therefore, due to (23), we immediately have that $\mathbf{curl}\,\Phi_h \subseteq Z_h$. On the other hand, Lemma 4.1 guarantees that for every $\mathbf{v}_h$ with $\operatorname{div}\mathbf{v}_h = 0$ there exists a unique $w_h \in \Phi_h$ such that $(\mathbf{curl}\, w_h)|_{\partial K} = \mathbf{v}_h|_{\partial K}$ for all $K \in \mathcal{T}_h$. Hence, from (23) there follows $\mathbf{curl}\, w_h = \mathbf{v}_h$ in Ω, i.e., $\mathbf{curl}\,\Phi_h = Z_h$.

□

In view of Proposition 4.1, the solution $\mathbf{u}_h \in V_h$ of (14) can be written as $\mathbf{u}_h = \mathbf{curl}\,\psi_h$ where $\psi_h \in \Phi_h$ solves

$$\begin{cases} \text{Find } \psi_h \in \Phi_h \text{ such that} \\ a_h(\mathbf{curl}\,\psi_h, \mathbf{curl}\,\varphi_h) =< \mathbf{f}, \mathbf{curl}\,\varphi_h >_h \qquad \forall \varphi_h \in \Phi_h. \end{cases} \tag{24}$$

We will refer to (24) as to the virtual stream-formulation of problem (2).

Note that, as an immediate consequence of Lemma 4.1, the kernel of the **curl** operator on the space Φ_h is given by the trivial space $\{0\}$. Therefore the strict positivity of $a_h(\cdot,\cdot)$ on V_h immediately reflects on the strict positivity of $a_h(\mathbf{curl}\,\cdot, \mathbf{curl}\,\cdot)$ on Φ_h. This implies the invertibility of the discrete linear system in (24). The convergence of the solution $\mathbf{u}_h = \mathbf{curl}\psi_h$ to $\mathbf{u}$ follows immediately from Theorem 3.1 and the equivalence between the two formulations.
Implementation issues. The implementation of the method (24) does not hide any particular difficulty. One first needs to build the local (element-wise) stiffness matrixes associated to the bilinear form $a_h^K(\cdot,\cdot)$, $K \in \mathcal{T}_h$, and the local vectors representing the loading term $< \mathbf{f}_h, \cdot >_h$ on K. This can be done identically to the mimetic method of [8, 10], or following the alternative way shown for the Laplace problem in [7]. The local stiffness matrixes associated to the bilinear form $a_h^K(\mathbf{curl}\,\cdot, \mathbf{curl}\,\cdot)$ are then built by introducing local matrixes $CURL_h$ that represent the **curl** operator in terms of the degrees of freedom of $V_{h|K}$ and $\Phi_{h|K}$. For instance, given any $\varphi_h \in \Phi_h$, the vertex values of $\mathbf{v}_h = \mathbf{curl}\,\varphi_h \in V_h$ can be immediately computed using the values of $\nabla\varphi_h$ at the same vertexes (which are, by definition, degrees of freedom of the space Φ_h). In a similar way, we observe that the value of $\mathbf{v}_h \cdot \mathbf{n}_e$ at the edge midpoint m_e of e can be computed as $\partial\varphi_h/\partial\mathbf{t}_e(\mathsf{m}_e)$; recalling that φ_h is a cubic function and using the Cavalieri-Simpson integration rule yield

$$\frac{\partial\varphi_h}{\partial\mathbf{t}_e}(\mathsf{m}_e) = \frac{3}{2|e|}\Big(\varphi_h(\mathsf{v}') - \varphi_h(\mathsf{v})\Big) - \frac{1}{4}\Big(\frac{\partial\varphi_h}{\partial\mathbf{t}_e}(\mathsf{v}') + \frac{\partial\varphi_h}{\partial\mathbf{t}_e}(\mathsf{v})\Big),$$

being v, v' the two (ordered) vertexes that are extrema for edge e. Note that the right-hand side of the above relation is expressed in terms of the degrees of freedom of Φ_h; i.e. of the vertex values of φ_h and $\nabla\varphi_h$.

Similar arguments apply to the construction of the loading vector.

5 Numerical tests

In this section we test our virtual stream method (24) and compare its numerical performance with the one of the classical scheme (14). Both scheme have been implemented using MATLAB. In the sequel, we consider two different benchmark problems defined on the computational domain $\Omega := (0,1)^2$ and we employ the following types of mesh (se also Figures 3-4):

- $\mathcal{T}_h^1$: Triangular mesh.
- $\mathcal{T}_h^2$: Structured hexagonal meshes.
- $\mathcal{T}_h^3$: Non-structured hexagonal meshes made of convex hexagons.
- $\mathcal{T}_h^4$: Regular subdivisions of the domain in $N \times N$ subsquares.

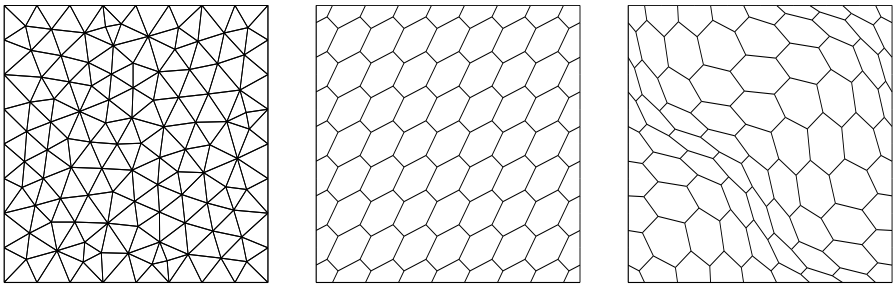

Figure 3: Sample meshes: $\mathcal{T}_h^1$ (left), $\mathcal{T}_h^2$ (middle) and $\mathcal{T}_h^3$ (right) for $h = 1/8$.

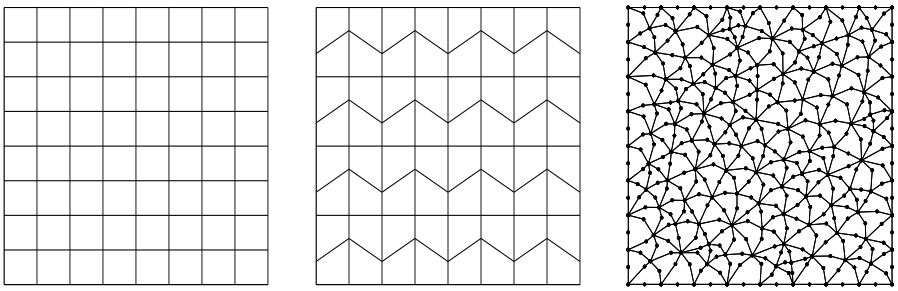

Figure 4: Sample meshes: $\mathcal{T}_h^4$ (left), $\mathcal{T}_h^5$ (middle) and $\mathcal{T}_h^6$ (right) for $h = 1/8$.

- $\mathcal{T}_h^5$: Trapezoidal meshes which consist of partitions of the domain into $N \times N$ congruent trapezoids, all similar to the trapezoid with vertexes $(0,0), (\frac{1}{2},0), (\frac{1}{2},\frac{2}{3})$, and $(0,\frac{1}{3})$.
- $\mathcal{T}_h^6$: Meshes built from $\mathcal{T}_h^1$ considering the middle point of each edge as a new vertex, that is then moved randomly; note that these meshes contain non-convex elements.

To test the convergence properties of the methods, we introduce the following discrete maximum norm: for any sufficiently regular function $\mathbf{v}$,

$$|||\mathbf{v}|||_{0,\infty} := \max_{\mathsf{v} \in \mathcal{V}_h} |\mathbf{v}(\mathsf{v})|_\infty \tag{25}$$

where $\mathcal{V}_h$ represents the set of vertexes of $\mathcal{T}_h$ and $|\cdot|_\infty$ denotes the l^∞ vector norm. We also introduce the following discrete H^1 like norm:

$$|||\mathbf{v}|||_{1,2} := \left(\sum_{e \in \mathcal{E}_h} h_e \left\| \frac{\partial \mathbf{v}}{\partial \mathbf{t}_e} \right\|_{0,e}^2 \right)^{1/2}. \tag{26}$$

Accordingly, we denote by

$$E_{0,\infty}^h := |||\mathbf{u} - \mathbf{u}_h|||_\infty \qquad E_{1,2}^h := |||\mathbf{u} - \mathbf{u}_h|||_{1,2}$$

the corresponding errors and we measure the experimental order of convergence as

$$R := \frac{\log(E/E')}{\log(h/h')},$$

where h and h' denote two consecutive meshsizes and E and E' denote the associated errors.

5.1 Stokes problem with analytical solution

The first benchmark problem is taken from [4]. Choosing $\nu = 1$ and the load $\mathbf{f}$ as:

$$\mathbf{f}(x,y) = \begin{bmatrix} -4\pi^2\cos(2\pi x)\sin(2\pi y) + 2\pi^2\sin(2\pi y) - y^2 \\ 4\pi^2\cos(2\pi y)\sin(2\pi x) - 2\pi^2\sin(2\pi x) - 2xy \end{bmatrix},$$

the solution $(\mathbf{u}, p)$ of problem (2) is given by:

$$u_1(x,y) = -\cos(2\pi x)\sin(2\pi y) + \sin(2\pi y),$$

$$u_2(x,y) = \sin(2\pi x)\cos(2\pi y) - \sin(2\pi x),$$

$$p(x,y) = xy^2 - \frac{1}{6}.$$

Table 1 shows the convergence history of the virtual velocity-pressure method (14) applied to our test problem with five different family of meshes, while Table 2 collects the corresponding results when the virtual stream formulation (24) is applied. The tables include the number of dofs, the number nnz of nonzero matrix elements, the convergence rates R, the total time TT(s) in seconds used for computing the approximate solutions, the discrete errors $E^h_{0,\infty}$ and $E^h_{1,2}$.

We note that the results reported in the tables confirm, for both methods, the first order convergence rate in the discrete H^1 like norm (in agreement with Theorem 3.1) and show a quadratic rate in the discrete L^∞ norm. This holds for all the considered meshes. Moreover, since the two methods are equivalent, it is not surprising to note that the error values reported in Table 1 and the corresponding ones of Table 2 are almost identical. The negligible discrepancy is related to the numerical round-off associated to the different sequence of computations performed by the two methods.

Finally, with the aim of performing a comparison between our novel virtual stream method and the virtual velocity-pressure method, we remark (see third column in Tables 1 and 2) that the number of degrees of freedom employed by the virtual stream method (24) is much smaller than the one used by the original scheme (14). For instance, in the triangular case the reduction factor is greater than two. Note that the reduction of the dofs has also important consequences on the number of nonzero elements in the matrixes (see the fourth column in Tables 1 and 2). Finally, although the comparison may be code depending, we report (last column in the tables) the total time needed by the two algorithms to assemble and solve the linear systems. Again the advantage of the virtual stream formulation is clear.

5.2 The lid-driven cavity problem

The second benchmark example is the so called lid-driven cavity problem which is a standard test problem, for which there is no exact solution, typically employed to validate numerical

Table 1: Approximation of the velocity $\mathbf{u}$: convergence analysis of the virtual velocity-pressure method (14).

Mesh	$1/h$	dof	nnz	$E^h_{0,\infty}$	$R_{0,\infty}$	$E^h_{1,2}$	$R_{1,2}$	TT(s)
$\mathcal{T}^1_h$	8	697	11558	8.7465e-2	–	2.3821e-0	–	1.36
	16	2952	52321	3.4740e-2	1.33	1.2100e-0	0.98	3.86
	32	12012	218947	7.7637e-3	2.16	6.2742e-1	0.95	18.81
	64	48899	903116	2.1290e-3	1.87	3.1602e-1	0.99	170.92
	128	198496	3690320	5.6025e-4	1.93	1.5800e-1	1.00	2075.83
$\mathcal{T}^2_h$	8	146	3781	7.6563e-1	–	3.7968e-0	–	0.34
	16	546	16620	3.9845e-1	0.94	2.1247e-0	0.84	0.59
	32	2114	68427	1.4242e-1	1.48	9.2731e-1	1.20	1.56
	64	8322	279846	4.0863e-2	1.80	3.7620e-1	1.30	6.53
	128	33026	1154059	1.0650e-2	1.94	1.6652e-1	1.18	93.90
$\mathcal{T}^3_h$	8	146	3851	9.2800e-1	–	3.9456e-0	–	0.34
	16	546	17117	5.8806e-1	0.66	2.5752e-0	0.62	0.63
	32	2114	71887	2.6751e-1	1.14	1.2899e-0	1.00	1.60
	64	8322	294709	9.2930e-2	1.53	5.1945e-1	1.31	6.78
	128	33026	1193617	2.6568e-2	1.81	2.0835e-1	1.32	57.7
$\mathcal{T}^4_h$	8	275	3960	5.4032e-1	–	3.0340e-0	–	0.43
	16	1187	19410	1.8201e-1	1.57	1.2733e-0	1.25	1.00
	32	4931	85284	5.0021e-2	1.86	5.4736e-1	1.22	3.71
	64	20099	356798	1.2863e-2	1.96	2.5782e-1	1.09	22.6
	128	81154	1433296	3.2361e-3	1.99	1.2669e-1	1.03	170.31
$\mathcal{T}^6_h$	8	339	9428	4.8894e-1	–	3.0986e-0	–	0.88
	16	1603	49412	1.5073e-1	1.70	1.6231e-0	0.93	1.99
	32	6771	218348	4.2964e-2	1.81	8.3954e-1	0.95	7.46
	64	27507	904488	1.0800e-2	1.99	4.3331e-1	0.95	54.50
	128	111875	3713168	2.3505e-3	2.20	2.1768e-1	0.99	684.78

methods for fluids (see, for instance [22, 28]). The 2D lid-driven cavity problem describes the flow in a rectangular container which is driven by the uniform motion of one lid.

The problem is set up with the following boundary condition: $\mathbf{u} = (1, 0)$ on the top lid and $\mathbf{u} = (0, 0)$ elsewhere, while the source function $\mathbf{f}$ is set equal to $\mathbf{0}$ and the viscosity ν equal to 1.

Due to the change of boundary conditions, two singularities appears at the top corners of the domain.

In the sequel, we report the numerical results obtained using the virtual stream formulation (24), where the following boundary conditions for the stream function ψ_h have been employed: $\nabla\psi_h = (0, 1)$ on the top lid and $\nabla\psi_h = (0, 0)$ elsewhere; $\psi_h = 0$ on the whole boundary.

We first employed a triangular mesh (family $\mathcal{T}^1_h$) with $h = 1/64$: Figure 5 reports the first and second velocity component profile, while Figure 6 shows the velocity field.

Table 2: Approximation of the velocity $\mathbf{u}$: convergence analysis of the virtual stream method (24).

Mesh	$1/h$	dof	nnz	$E^h_{0,\infty}$	$R^h_{0,\infty}$	$E^h_{1,2}$	$R^h_{1,2}$	TT(s)
$\mathcal{T}_h^1$	8	273	5031	8.7466e-2	–	2.3822e-0	–	1.19
	16	1212	24102	3.4752e-2	1.33	1.2100e-0	0.98	3.38
	32	5040	103140	7.7743e-3	2.16	6.2742e-1	0.95	14.14
	64	20739	429867	2.1300e-3	1.87	3.1602e-1	0.99	99.92
	128	84633	1765593	5.6141e-4	1.92	1.5800e-1	1.00	1461.64
$\mathcal{T}_h^2$	8	96	2672	7.6296e-1	–	3.7972e-0	–	0.30
	16	384	12710	3.9766e-1	0.94	2.1249e-0	0.84	0.55
	32	1536	55158	1.4217e-1	1.48	9.2737e-1	1.20	1.38
	64	6144	229518	4.0791e-2	1.80	3.7621e-1	1.30	5.43
	128	24576	939300	1.0632e-2	1.94	1.6652e-1	1.17	33.65
$\mathcal{T}_h^3$	8	96	2676	9.2770e-1	–	3.9448e-0	–	0.25
	16	384	12762	5.8785e-1	0.66	2.5750e-0	0.62	0.42
	32	1536	55386	2.6743e-1	1.14	1.2899e-0	1.00	1.15
	64	6144	230490	9.2912e-2	1.53	5.1943e-1	1.31	4.16
	128	24576	940122	2.6563e-2	1.81	2.0835e-1	1.32	27.03
$\mathcal{T}_h^4$	8	147	2065	5.3945e-1	–	3.0340e-0	–	0.45
	16	675	11123	1.8179e-1	1.57	1.2733e-0	1.25	0.88
	32	2883	50705	4.9967e-2	1.86	5.4736e-1	1.22	3.03
	64	11907	215651	1.2849e-2	1.96	2.5782e-1	1.09	14.09
	128	48387	897833	3.2327e-3	1.99	1.2669e-1	1.03	130.76
$\mathcal{T}_h^6$	8	243	6705	4.8976e-1	–	3.0986e-0	–	1.05
	16	1179	36765	1.5089e-1	1.70	1.6231e-0	0.93	1.85
	32	5031	165843	4.2963e-2	1.81	8.3953e-1	0.95	6.74
	64	20535	692937	1.0816e-2	1.99	4.3331e-1	0.96	42.22
	128	83715	2856303	2.3514e-3	2.20	2.1768e-1	0.99	495.53

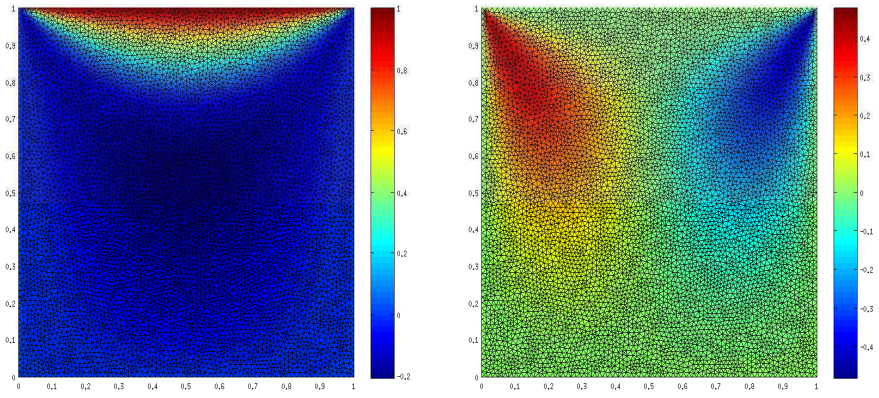

Figure 5: The first and second velocity component profile for the lid-driven cavity problem obtained with a triangular mesh (family $\mathcal{T}_h^1$, $h = 1/64$).

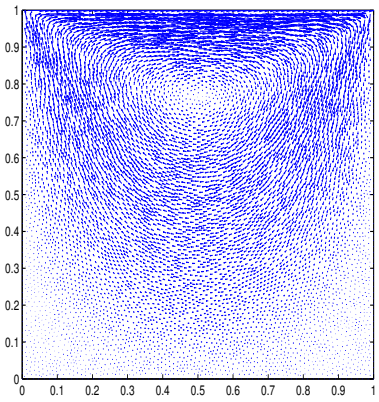

Figure 6: The velocity profile for the lid-driven cavity problem obtained with a triangular mesh (family $\mathcal{T}_h^1$, $h = 1/64$).

The second set of experiments have been run on trapezoidal mesh (family $\mathcal{T}_h^5$) with $h = 1/64$. Figure 7 shows the first and second velocity component profile, and Figure 8 shows the velocity field.

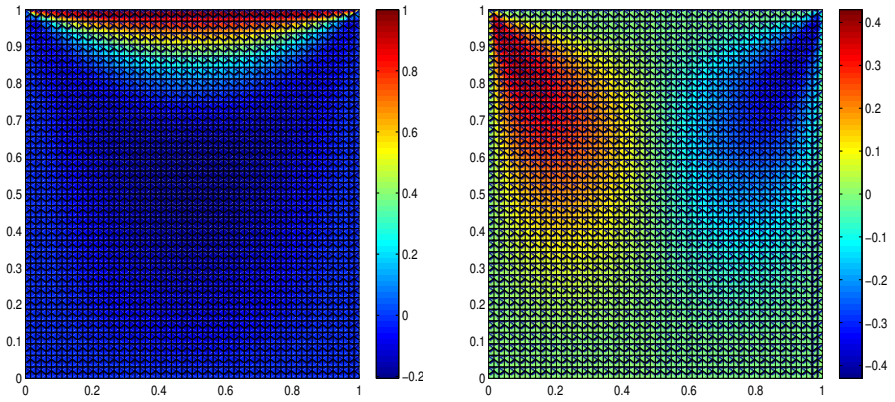

Figure 7: The first and second velocity component profile for the lid-driven cavity problem obtained with a trapezoidal mesh (family $\mathcal{T}_h^5$, $h = 1/64$).

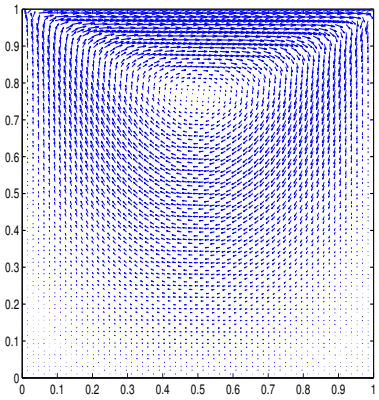

Figure 8: The velocity profile for the lid-driven cavity problem obtained with a trapezoidal mesh (family $\mathcal{T}_h^5$, $h = 1/64$).

The results obtained are in full agreement with those of [22, 28] and show both the stability and accuracy of our new virtual stream method also in the presence of jumping boundary conditions.

References

[1] P. F. Antonietti, L. Beirão da Veiga, C. Lovadina and M. Verani. Hierarchical a posteriori error estimators for the mimetic discretization of elliptic problems. *SIAM J. Numer. Anal.*, 2013. To appear.

[2] P. F. Antonietti, L. Beirão da Veiga, and M. Verani. A mimetic discretization of elliptic obstacle problems. *Math. Comp.*, 2013, doi: 10.1090/S0025-5718-2013-02670-1 .

[3] P. F. Antonietti, N. Bigoni, and M. Verani. A mimetic discretization of elliptic control problems. *J. Sci. Comput.*, 2012. doi: 10.1007/s10915-012-9659-7.

[4] F. Auricchio, L. Beirão da Veiga, C. Lovadina and A. Reali. An analysis of some mixed-enhanced finite element for plane linear elasticity. *Comput. Methods Appl. Mech. Engrg.* 194:2947–2968, 2005.

[5] L. Beirão da Veiga. A residual based error estimator for the mimetic finite difference method. *Numer. Math.*, 108(3):387–406, 2008.

[6] L. Beirão da Veiga, F. Brezzi and L.D. Marini. Virtual Elements for linear elasticity problems. *SIAM J. Numer. Anal.*, 2013. To appear.

[7] L. Beirão da Veiga, F. Brezzi, A. Cangiani, G. Manzini, L.D. Marini and A. Russo. Basic Principles of Virtual Element Methods. *Math. Models Methods Appl. Sci.*, 23(1):199–214, 2013.

[8] L. Beirão da Veiga, V. Gyrya, K. Lipnikov and G. Manzini. Mimetic finite difference method for the Stokes problem on polygonal meshes. *J. Comput. Phys.*, 228:7215–7232, 2009.

[9] L. Beirão da Veiga and K. Lipnikov. A mimetic discretization of the Stokes problem with selected edge bubbles. *SIAM J. Sci. Comp.*, 32:875–893, 2010.

[10] L. Beirão da Veiga, K. Lipnikov and G. Manzini. Error Analysis for a Mimetic Discretization of the Steady Stokes Problem on Polyhedral Meshes. *SIAM J. Numer. Anal.*, 48(4):1419–1443, 2010.

[11] L. Beirão da Veiga and G. Manzini. A virtual element method with arbitrary regularity. *IMA J. Numer. Anal.*, 2013. To appear.

[12] L. Beirão da Veiga and D. Mora. A mimetic discretization of the Reissner-Mindlin plate bending problem. *Numer. Math.*, 117(3):425–462, 2011.

[13] S. C. Brenner and R. L. Scott *The mathematical theory of finite element methods.* Texts in Applied Mathematics, 15. Springer-Verlag, New York, 2008.

[14] F. Brezzi, A. Buffa, and K. Lipnikov. Mimetic finite differences for elliptic problems. *M2AN Math. Model. Numer. Anal.*, 43(2):277–295, 2009.

[15] F. Brezzi and M. Fortin. *Mixed and Hybrid Finite Element Methods.* Springer-Verlag, New York, 1991.

[16] F. Brezzi, K. Lipnikov, and M. Shashkov. Convergence of mimetic finite difference method for diffusion problems on polyhedral meshes. *SIAM J. Num. Anal.*, 43:1872–1896, 2005.

[17] F. Brezzi, K. Lipnikov, and V. Simoncini. A family of mimetic finite difference methods on polygonal and polyhedral meshes. *Math. Models Methods Appl. Sci.*, 15:1533–1553, 2005.

[18] F. Brezzi and L.D. Marini. Virtual elements for plate bending problems. *Comput. Methods Appl. Mech. Engrg.*, 253:455–462, 2012

[19] Z. Cai, C. Tong, P. S. Vassilevski, and C. Wang. Mixed finite element methods for incompressible flow: Stationary Stokes equations. *Numer. Methods Partial Differential Equations*, 26(4):957–978, 2010.

[20] P. G. Ciarlet. *The Finite Element Method for Elliptic Problems*. North-Holland, 1978.

[21] V. Girault and P.A. Raviart. *Finite element methods for Navier-Stokes equations.* Springer-Verlag, Berlin, 1986.

[22] L. P. Franca, S. Frey and T.J.R. Hughes. Stabilized finite element methods: I. Application to the advective-diffusive model. *Comput. Meth. Appl. Mech. Engrg.* 95:253–276, 1992.

[23] K. Lipnikov, G. Manzini and M. Shashkov. Mimetic finite difference method. Review paper, submitted for publication.

[24] A. Tabarraei and N. Sukumar. Conforming polygonal finite elements. *Int. J. Numer. Meth. Engrg.*, 61(12):2045–2066, 2004.

[25] A. Tabarraei and N. Sukumar. Extended finite element method on polygonal and quadtree meshes. *Comput. Methods Appl. Mech. Engrg.*, 197(5):425–438, 2007.

[26] C. Talischi, G.H. Paulino, A. Pereira A. and I.F.M. Menezes. Polygonal finite elements for topology optimization: A unifying paradigm. *Int. J. for Num. Meth. Engnr.*, 82:671–698, 2010.

[27] C. Talischi, G.H. Paulino, A. Pereira A. and I.F.M. Menezes. PolyTop: a Matlab implementation of a general topology optimization framework using unstructured polygonal finite element meshes *J. of Struct. and Mult. Optim.*, 45:329–357, 2012.

[28] J. Wang, Y. Wang and X. Ye. A robust numerical method for Stokes equations based on divergence-free H(div) finite element methods. *SIAM J. Sci. Comput.*, 31(4):2784–2802, 2009.

MOX Technical Reports, last issues

Dipartimento di Matematica "F. Brioschi",
Politecnico di Milano, Via Bonardi 9 - 20133 Milano (Italy)

10/2013 Antonietti, P.F.; Beirao da Veiga, L.; Mora, D.; Verani, M.
A stream virtual element formulation of the Stokes problem on polygonal meshes

09/2013 Vergara, C.; Palamara, S.; Catanzariti, D.; Pangrazzi, C.; Nobile, F.; Centonze, M.; Faggiano, E.; Maines, M.; Quarteroni, A.; Vergara, G.
Patient-specific computational generation of the Purkinje network driven by clinical measuraments

08/2013 Chen, P.; Quarteroni, A.; Rozza, G.
A Weighted Reduced Basis Method for Elliptic Partial Differential Equations with Random Input Data

07/2013 Chen, P.; Quarteroni, A.; Rozza, G.
A Weighted Empirical Interpolation Method: A-priori Convergence Analysis and Applications

06/2013 Ded, L.; Quarteroni, A.
Isogeometric Analysis for second order Partial Differential Equations on surfaces

05/2013 Caputo, M.; Chiastra, C.; Cianciolo, C.; Cutri , E.; Dubini, G.; Gunn, J.; Keller, B.; Zunino, P.;
Simulation of oxygen transfer in stented arteries and correlation with in-stent restenosis

04/2013 Morlacchi, S.; Chiastra, C.; Cutr, E.; Zunino, P.; Burzotta, F.; Formaggia, L.; Dubini, G.; Migliavacca, F.
Stent deformation, physical stress, and drug elution obtained with provisional stenting, conventional culotte and Tryton-based culotte to treat bifurcations: a virtual simulation study

03/2013 Antonietti, P.F.; Ayuso de Dios, B.; Bertoluzza, S.; Pennacchio, M.
Substructuring preconditioners for an $h-p$ Nitsche-type method

02/2013 Brugiapaglia, S.; Gemignani, L.
On the simultaneous refinement of the zeros of H-palindromic polynomials

01/2013 Arnold, D.N.; Boffi, D.; Bonizzoni,F.
Tensor product finite element differential forms and their approximation properties